Properties of a Dimer of $tRNA_I^{Tyr}$ (*Escherichia coli*)†

S. K. Yang, D. G. Söll, and D. M. Crothers*

ABSTRACT: Tyrosine-specific tRNA from *Escherichia coli* can be converted to a dimer by heating at 50° in buffer containing 0.5 M Na^+, but no Mg^{2+}, a conversion that can be reversed at higher temperature. The dimer does not accept tyrosine in the usual charging assay. The thermal melting transition measured at the 4-thiouridine absorbance band indicates that the dimer does not have the monomer tertiary structure. Its heat of melting to monomer is about 135 kcal/mole of dimer. By summing the slow kinetic effects due to this conversion, we found that the absorbance at 260 nm increases by 3.8% when the dimer melts to monomer. In other kinetic experiments we found that the rate constant for dimer formation is three to four orders of magnitude slower than for dimerization of self-complementary oligonucleotides; the apparent activation energy for dimer formation is slightly negative. We propose that $tRNA_I^{Tyr}$ (*E. coli*) dimerizes through self-complementarity in the pseudouridine loop and also in the dihydrouridine loop. This structure contrasts with that proposed by Loehr and Keller for chargeable dimers of $tRNA_{Iab}^{Ala}$ (yeast). We suggest a slight modification of their proposal to account for all the observations.

The problem of interaction among natural RNAs is virtually unexplored, even though there are several important questions relating to function that could involve such an interaction. For example, does tRNA interact with rRNA in the course of its function? Is it possible for control of RNA function to be exerted by interaction with other oligo- or polyribonucleotides? A model system for examining the general physical mechanism of such processes is the reaction between two tRNA molecules to produce a dimer. We have found that a specific dimer is formed from $tRNA_I^{Tyr}$ (*Escherichia coli*) under conditions that allow us to study thermodynamics, kinetics, and also structural changes as revealed by spectroscopy.

Aggregation of tRNA is often observed in the course of preparative procedures, storage, or heating and cooling. For example, Brown and Zubay (1960) found association of unfractionated aminoacyl-tRNA after heating and cooling in low ionic strength, neutral buffer. Schleich and Goldstein (1964) detected nonchargeable aggregates of $tRNA^{Ala}$ (*E. coli*) from the low partition coefficient fractions of countercurrent separation; the amino acid acceptor activity could be recovered by heating in urea. Inactive fractions of *E. coli* tRNA, eluting early from Sephadex columns and presumably aggregates, were found by Röschenthaler and Fromageot (1965). Again the activity could be increased by heating or by dialysis against low salt buffers. Söll *et al.* (1967) observed aggregates of glycyl-$tRNA^{Gly}$ (*E. coli*), glycyl-$tRNA^{Gly}$ (yeast), seryl-$tRNA^{Ser}$ (*E. coli*), and alanyl-$tRNA^{Ala}$ (*E. coli*), which could be converted to the coresponding monomeric species by short heat treatment. Stable inactive dimers and higher aggregates from ethanol precipitation of $tRNA^{Gly}$ (yeast), which could also be converted to monomers by a short heat treatment, were demonstrated by Hampel, *et al.* (1971). Partialy active aggregates of $tRNA^{Ser}$ (yeast) were demonstrated by Adams and Zachau (1968); the activity could be recovered by heat treatment.

In contrast to these inactive or partially active aggregates, Loehr and Keller (1968) isolated fully active dimers of $tRNA^{Ala}$ (yeast). Dimers could be prepared by heating the tRNA in concentrated solution, and dissociated by heat treatment in dilute solution.

In the experiments reported here we show that heat treatment of concentrated solutions of $tRNA_I^{Tyr}$ (*E. coli*) leads to a nonchargeable species with dimer molecular weight; dissociation can be accomplished by heat treatment under appropriate conditions. We report equilibrium, kinetic, and centrifugation studies of the dimer.

The key questions in considering the aggregation phenomenon are two. What is the structural basis, and why are some aggregates chargeable and others not? In interpreting our results we focus on the contrast between our inactive dimer preparation and the chargeable dimers of Loehr and Keller (1968). Both of these species are formed under annealing conditions, and are therefore the state of minimum free energy under appropriate conditions. A structural model for the dimer must explain why the two tRNAs of differing sequence form dimers of distinctly differing properties.

Materials and Methods

tRNA. E. coli K12 (CA244) $tRNA_I^{Tyr}$ was purified from the fractions of the first $tRNA^{Tyr}$ peak of a BD-cellulose column (Armstrong *et al.*, 1969) by DEAE-Sephadex A50 column with a linear salt gradient (Nishimura *et al.*, 1967). The pooled fractions were concentrated on a DEAE-cellulose column and precipitated with ethanol. The precipitates were stored in the freezer until use. The final tRNA preparation had a specific activity of 1650 pmoles/A_{260} unit, which is estimated to be 97% pure.[1]

Assay for Tyrosine Acceptor Activity. Acceptor activity assays were performed as described by Söll *et al.* (1967). [^{14}C]Tyrosine was obtained from New England Nuclear with a specific activity of 364 Ci/mole.

Buffer Systems. Experiments were carried out in buffers containing phosphate, cacodylate, EDTA, and perchlorate,

† From the Departments of Chemistry, Molecular Biophysics, and Biochemistry, Yale University, New Haven, Connecticut 06520. *Received December 20, 1971.* This research was supported by a grant (GM 12589) from the National Institutes of Health. D. M. C. holds a Career Development award (GM 19978) from the same source.

[1] One A_{260} unit of tRNA is assumed to be 1.7 nmoles.

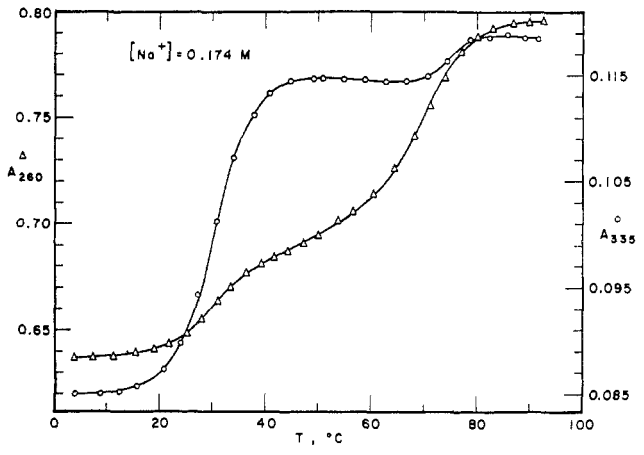

FIGURE 1: Melting curves of $tRNA_I^{Tyr}$ in 0.17 PCEP at 260 nm (Δ, left axis) and 335 nm (○, right axis). See Materials and Methods for experimental details.

pH 7, designated 0.17 PCEP[2] and 0.5 PCEP;[2] the numerical value in front of PCEP indicates the molar concentration of Na^+.

Ultraviolet Melting of $tRNA_I^{Tyr}$. The melting curves of $tRNA_I^{Tyr}$ were measured on a Cary 14 recording spectrophotometer equipped with a thermostated cell compartment. An appropriate amount of the concentrated $tRNA_I^{Tyr}$ was transfered with a micropipet, diluted with glass-distilled water, and then dialyzed extensively against distilled water and 1 mM Na_2EDTA in the cold to remove any contaminants of divalent ions. It was then dialyzed against 0.17 PCEP or 0.5 PCEP in the cold with three changes of buffer. Each dialysis was carried out for at least 5 hr. The dialyzed sample was degassed by bubbling helium through the solution for a few minutes and then was transfered to a 1-cm path-length, Teflon-stoppered, and water-jacketed cell connected to a constant-temperature bath. The sample cell temperature was calibrated by measuring the temperature difference between the bath and cell, with the spectrophotometer compartment kept at 25° by another constant-temperature bath. For each bath temperature, the cell temperature was measured by inserting a thermistor (Victory Engineering, T33A35) through the Teflon stopper into the cell filled with buffer. The gap between the thermistor and the stopper was sealed with General Electric Co. RTV 60 silicone rubber. The same conditions were used for all the measurements with the Cary 14, so that it was not necessary to place the thermistor in contact with the sample. The cell temperature can be determined to ±0.1° with this arrangement.

Formation of $tRNA_I^{Tyr}$ Aggregates. $tRNA_I^{Tyr}$ in 0.5 PCEP (*ca.* 6 A_{260}/ml) was heated in a tightly stoppered test tube at 50° for 4 hr and then rapidly quenched in ice water. The quenched sample was stored in the freezer until use. For melting and sedimentation experiments, the sample was thawed and diluted with cold 0.5 PCEP to an appropriate concentration.

Ultracentrifuge Measurements. A Spinco Model E analytical ultracentrifuge equipped with ultraviolet optics and a photoelectric scanner was used for all sedimentation velocity and sedimentation equilibrium measurements. All runs were made in a 12-mm Epon double-sector cell at a concentration of about 0.5 A_{260}/ml in 0.5 PCEP. The density of 0.5 PCEP was measured with a pyconometer and its viscosity with a Cannon-Ubbelohde viscometer.

Melting of Dimers by Temperature-Jump Techniques. To resolve the slow-melting component of the dimers in 0.5 PCEP between 48 and 67°, a Y-shaped glass joint connected to two water baths was used to change the temperature of the spectrophotometer cell. After switching the bath to a new temperature, thermal equilibrium is reached in about 100 sec. The absorbance change of the slow-melting component for a temperature jump was then found by plotting the logarithm of absorbance *vs.* time. Several successive temperature jumps were performed to measure the total melting curve of the dimer until the slow-melting component had disappeared.

Results

The results we report below show that there is a heat-induced aggregation of $tRNA_I^{Tyr}$ (*E. coli*), which can be reversed under certain conditions. The main product is a dimer, and the dimer does not accept tyrosine in the usual assay. We measured kinetics and equilibria for the transition between monomer and dimer, and evaluated the enthalpy and activation energies on the basis of a two-state model (monomer and dimer). Preliminary experiments show that $tRNA_{II}^{Tyr}$ undergoes dimerization in the same way as $tRNA_I^{Tyr}$.

Phenomena That Indicate Heat-Induced Aggregation. IRREVERSIBLE MELTING CURVES OF $tRNA_I^{Tyr}$ IN 0.17 PCEP. *E. coli* $tRNA^{Tyr}$ has two 4-thiouridine residues next to each other in the nucleotide chain (Lipsett and Doctor, 1967; RajBandary *et al.*, 1969). These 4-thiouridine residues, absorbing maximally at around 335 nm, provide a probe to study the structure of $tRNA^{Tyr}$. Figure 1 shows the melting curves of $tRNA_I^{Tyr}$ in 0.17 PCEP at 260 and 335 nm. They are biphasic at both wavelengths with the T_m at 335 nm slightly higher than at 260 nm. In a solution of somewhat higher ionic strength, Seno *et al.* (1969) reported two similar hyperchromic transitions at 335 nm for $tRNA_{II}^{Tyr}$ (*E. coli* B), with the first T_m at around 50°. Since the only difference in the primary structure between $tRNA_I^{Tyr}$ and $tRNA_{II}^{Tyr}$ is in two residues in the extra arm of the cloverleaf structure (Goodman *et al.*, 1968), we would expect to observe similar melting behavior.[3] We found the first T_m to be about 30° at 335 nm in 0.17 PCEP. This considerably lower value cannot be accounted for by the small difference in ionic strength. The high T_m observed by Seno *et al.* (1969) may have been caused by the presence of some divalent ions from the inorganic salts (our buffer contains EDTA). At 335 nm, the first transition of $tRNA_I^{Tyr}$ in 0.17 PCEP constitutes 88% of the total absorbance increase in contrast to about 60% observed by Seno *et al.* (1969).

In order to test the reversibility of the first melting transition, the sample in 0.17 PCEP was melted to about 50°, then

[2] Abbreviations used are: 0.17 PCEP, buffer containing 0.39 mM NaH_2PO_4–0.61 mM Na_2HPO_4–10 mM $(CH_3)_2AsO_2Na$–1 mM Na_2EDTA–0.16 M $NaClO_4$, pH 7.0; 0.5 PCEP, buffer containing 0.39 mM NaH_2PO_4–0.61 mM Na_2HPO_4–10 mM $(CH_3)AsO_2Na$–1 mM Na_2EDTA–0.49 M $NaClO_4$, pH 7.0. A_λ is the absorbance of a solution, 1-cm path length, at wavelength λ.

[3] We recently found a similar T_m for the first melting transition at 335 nm for $tRNA_I^{Tyr}$ and $tRNA_{II}^{Tyr}$; there are differences in detail that will be reported later (S. K. Yang and D. M. Crothers, paper in preparation).

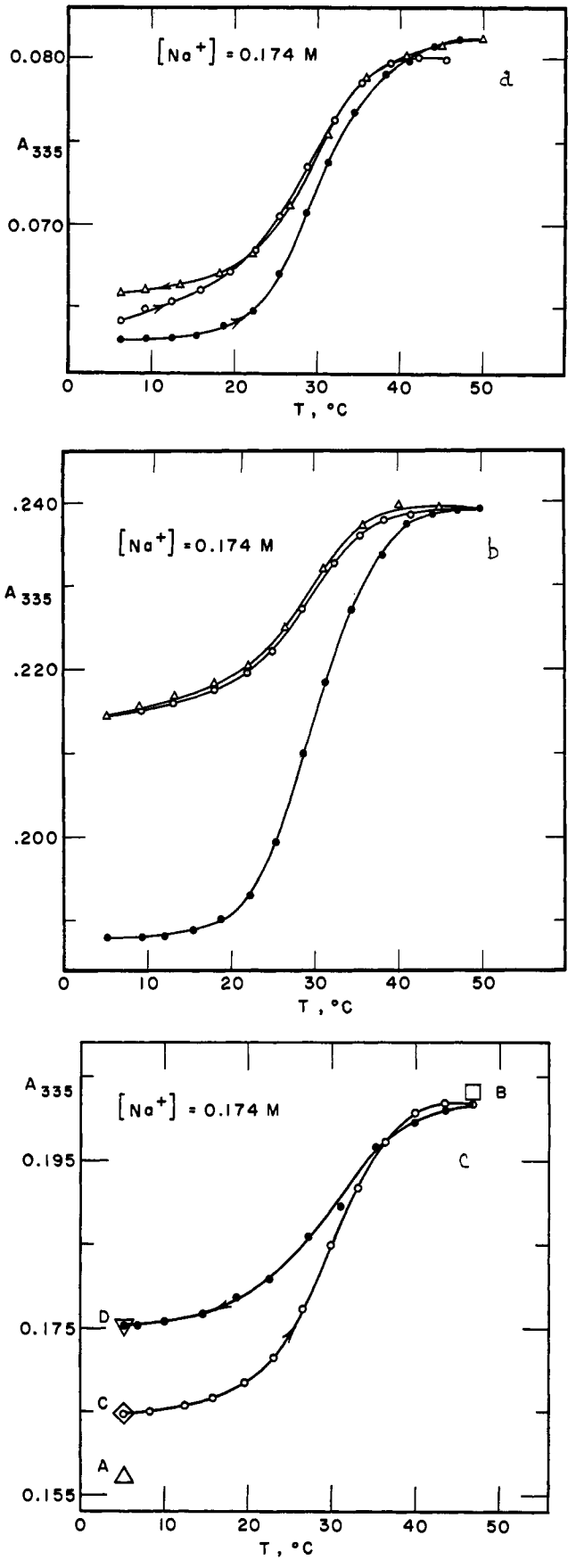

FIGURE 2: Reversibility of melting of $tRNA_I^{Tyr}$ in 0.17 PCEP at 335 nm; a and b are identical experiments except for tRNA concentration. The sample was first melted to about 50° (●) and cooled down gradually (△). It was left in the cell and kept in the refrigerator for 11 hr and remelted (○). (c) The absorbance of the sample was measured at 5° (point A) and it was then rapidly heated to 47° (point B). After the absorbance had reached a steady value at 47°, the sample was rapidly cooled to 5° (point C). After this treatment, the sample was remelted to 47° (○) and cooled down gradually (●) to 5° (point D).

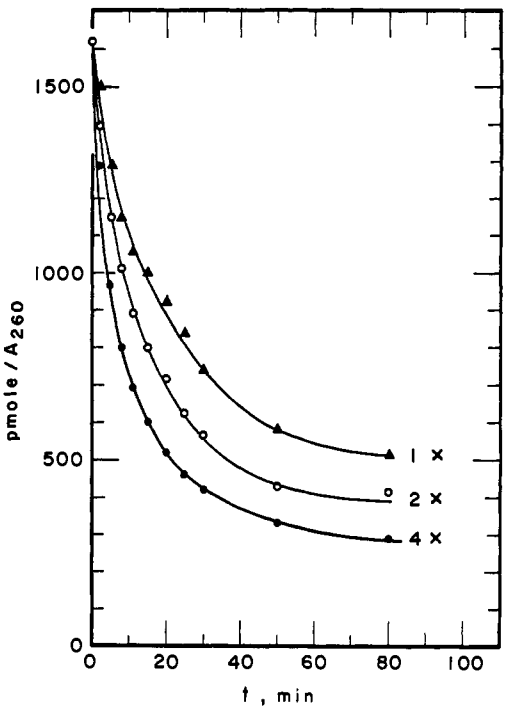

FIGURE 3: Inactivation of $tRNA_I^{Tyr}$ in 0.5 PCEP induced by heating. Three different concentrations of $tRNA_I^{Tyr}$ in 0.5 PCEP (200 μl each) were preheated at 50°. Samples (15 μl) were removed and cooled rapidly in an ice-cold test tube at each indicated time. Each preheated aliquot was assayed for its tyrosine acceptor activity (pmole/A_{260}). The concentrations of these three samples are: $1X$ = 0.73 A_{260}/ml, $2X$ = 1.45 A_{260}/ml, $4X$ × 2.9 A_{260}/ml.

cooled down gradually to obtain the reverse transition curve. At 260 nm, the upward and downward melting curves were almost superimposable. But at 335 nm, the change was not fully reversible. Figure 2a and 2b show the concentration dependence of the irreversibility. The absorbance of the once-melted sample did not drop back to its original value even when the sample was kept in the refrigerator for more than 11 hr. In Figure 2c, the sample was first melted from 5° (point A) by rapid heating to 47° (point B) and when the absorbance had reached a steady reading, it was then rapidly cooled down to 5° (point C). The absorbance of the quenched sample (point C) was higher than that of the unmelted sample (point A). But when it was remelted and cooled down gradually to this low temperature (point D), the absorbance was higher than both of the previous low-temperature values. Our interpretation of these results is that partial aggregation has occurred after the native $tRNA_I^{Tyr}$ has been melted to about 50°. Aggregation is more extensive in a slowly cooled sample.

INACTIVATION OF $tRNA_I^{Tyr}$ IN 0.5 PCEP INDUCED BY HEATING. Three different concentrations of $tRNA_I^{Tyr}$ in 0.5 PCEP were heated at 50°. Aliquots of each sample were transferred with a micropipet into ice-cold test tubes at different stages of heating. Each chilled sample was then assayed for amino acid acceptor activity. The results (Figure 3) show that inactivation is concentration dependent, again supporting the idea that there is aggregation induced by heating.

$tRNA_I^{Tyr}$ Aggregates Can Be Reactivated. Aggregates of tRNAs can generally be converted to their monomers by heating above 60°, followed by rapid cooling, either in the presence or absence of Mg^{2+} (Söll *et al.*, 1967; Brown and Zubay, 1960; Röschenthaler and Fromageot, 1965; Loehr

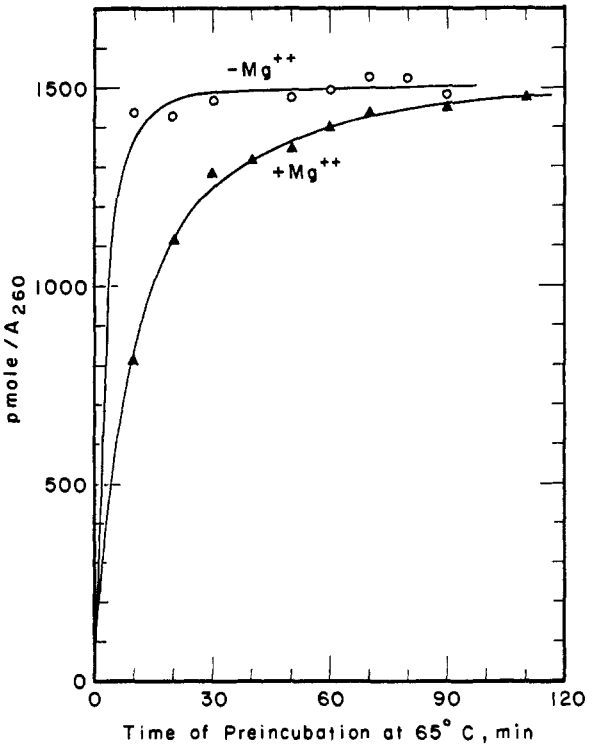

FIGURE 4: Reactivation of $tRNA_I^{Tyr}$ aggregates. The $tRNA_I^{Tyr}$ aggregate sample in 0.5 PCEP was heated at 65° for the indicated time. At each stage of heating, an aliquot was transfered to an ice-cold test tube. All alqiuots were then assayed for their tyrosine acceptor activities (pmole/A_{260}). The $tRNA_I^{Tyr}$ aggregate sample in 0.5 PCEP was diluted with concentrated sodium cacodylate buffer (pH 7.2) and $MgCl_2$ to a final concentration of 0.5 M Na^+ and 0.01 M Mg^{2+}. The experiment was carried out in the same way as described above. In both cases the final tRNA concentration was 0.42 A_{260}/ml.

and Keller, 1968; Adams and Zachau, 1968; Zachau, 1968). Aggregates can also be converted to monomers through urea and heat treatments (Schleich and Goldstein, 1964). The highly inactive aggregates of $tRNA_I^{Tyr}$ formed by heating the native material at 50° in 0.5 PCEP for 4 hr could also be reactivated by heat treatment, either in 0.5 PCEP alone or in 0.5 PCEP plus 10 mM Mg^{2+}. The reactivation was achieved, as shown in Figure 4, by heating the aggregated sample at 65°, followed by rapid cooling prior to the tyrosine acceptor

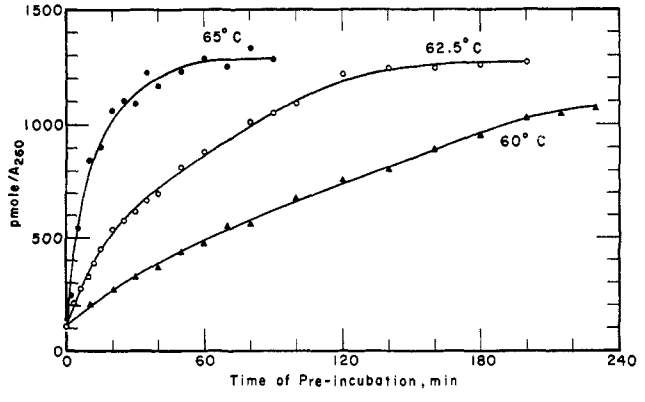

FIGURE 5: Reactivation of $tRNA_I^{Tyr}$ aggregates (0.59 A_{260}/ml) in the presence of Mg^{2+}. The experiment was carried out as described for the solid-triangle curve in Figure 4, using a variable temperature of preincubation.

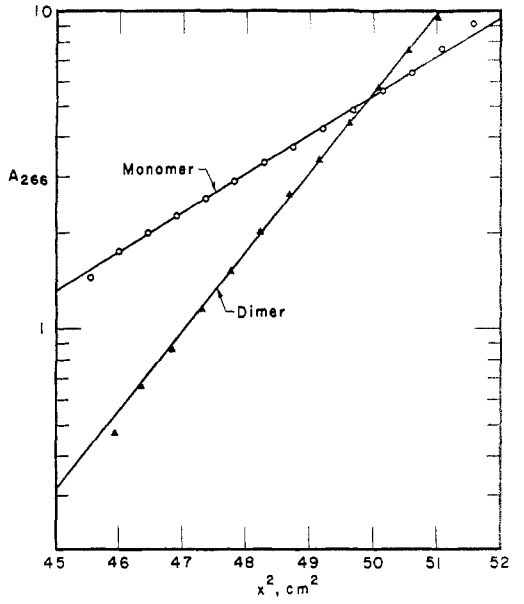

FIGURE 6: Plot of ln C *vs.* X^2 for sedimentation equilibrium runs of monomer and dimer $tRNA_I^{Tyr}$ in 0.5 PCEP, measured at 4° and 9945 rpm. The slope of monomer is 0.283 cm^{-2} and that of dimer is 0.570 cm^{-2}.

activity assays. It was found (Figure 4) that in the absence of Mg^{2+}, the reactivation can be achieved faster than that in the presence of Mg^{2+}. Presumably the presence of Mg^{2+} has stabilized the $tRNA_I^{Tyr}$ aggregates.

The reactivation in the presence of Mg^{2+} ions was further studied at different temperatures. The results are shown in Figure 5. The rate of reactivation increases as the temperature of reincubation increases. A crude estimate of the activation energy for this process from the temperature dependence of the half-time of maximal charging is $+130 \pm 15$ kcal/mole.

The maximal acceptor activities obtained in Figure 5 were variable and below the charging level of the native $tRNA_I^{Tyr}$. This discrepancy may have been caused by nonenzymatic hydrolysis at these temperatures in the presence of high concentration of Mg^{2+} ions, or by nuclease contamination.

The Main Product of the Aggregation Reaction Is a Dimer. EQUILIBRIUM SEDIMENTATION. To determine the extent of aggregation of $tRNA_I^{Tyr}$ under these conditions, we compared the sedimentation equilibrium molecular weights of monomer and aggregate. The apparent molecular weight, M_{app}, is defined by

$$M_{app} = \frac{2RT}{(1 - \bar{v}\rho)\omega^2} \frac{d \ln c}{dx^2} \quad (1)$$

where R is the gas constant, T the absolute temperature, ρ the density of the solution, $\bar{v} = 0.506$ (Adams *et al.*, 1967) the partial specific volume of the tRNA, ω the angular velocity, and c the concentration of tRNA at distance x from the axis of rotation. Because tRNA is a polyelectrolyte, M_{app} will not be exactly equal to the actual molecular weight (Johnson *et al.*, 1954; Tanford, 1961). Further deviations from ideal behavior may also result from preferential interaction of one of the solvent components (water and salt) with the RNA (Casassa and Eisenberg, 1964; Scheffler *et al.*, 1968). The measured M_{app} of the monomeric tRNA is (Ta-

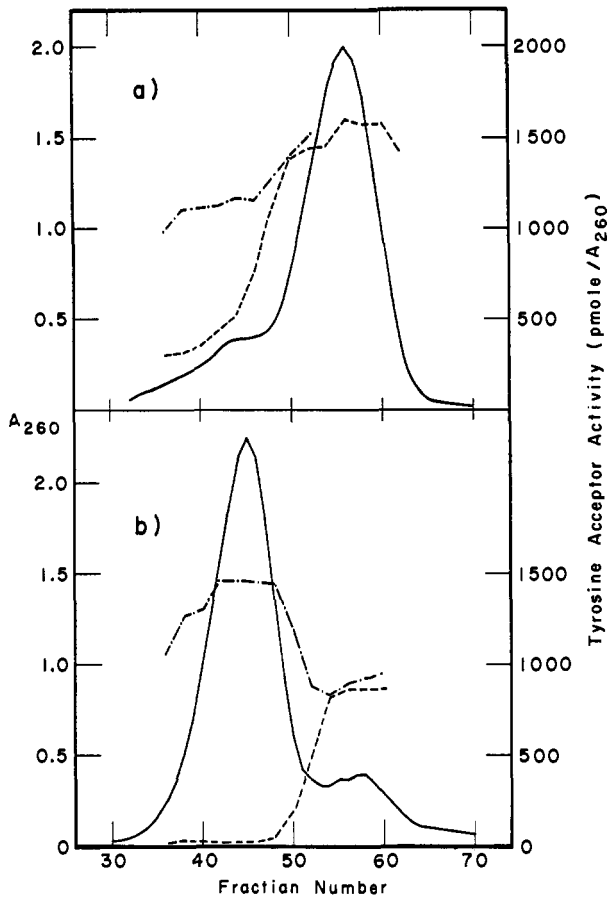

FIGURE 7: Gel filtration of $tRNA_I^{Tyr}$ monomers and dimers. A column (1 × 110 cm) of Sephadex G-100 was equilibrated and eluted with 0.49 M NaCl, 0.01 M sodium cacodylate (pH 7.0), and 1 mM Na_2EDTA at room temperature. The $tRNA^{Tyr}$ sample concentration was 47 A_{260}/ml in the column equilibration buffer. (a) A sample of 0.5 ml was directly loaded onto the column. (b) A 0.5-ml sample was loaded after the sample had been heated in a sealed test tube at 50° for 2.5 hr and immediately quenched in ice water. The sample was a mixture of $tRNA_I^{Tyr}$ (80%) and $tRNA_{II}^{Tyr}$ (20%) and had a tyrosine acceptor activity of 1300 pmole/A_{260} unit. The flow rate of the column was 9 ml/hr, and 1-ml fractions were collected. (—) Absorbance reading of elution profile; (- - -) tyrosine acceptor activities of the column fractions; (-·-) tyrosine acceptor activities of the column fractions after preincubation at 70° for 5 min.

ble I) 25,400, whereas the molecular weight computed for the sodium salt from the known sequence is 2.94×10^4. Therefore, the correction factors that must be applied to M_{app} to determine M amount to about 14%.

It seems safe to assume that $\bar{v}$ and the correction factors will be similar for monomer and aggregate. Hence we approximate the ratio of molecular weights for aggregate and monomer by setting

$$\frac{M_{aggregate}}{M_{monomer}} = \frac{(d \ln c/dx^2)_{aggregate}}{(d \ln c/dx^2)_{monomer}} \quad (2)$$

Figure 6 shows plots of d ln c/dx^2 for monomer and aggregate samples. (The aggregate had acceptor activity of 77 pmoles/A_{260} unit, which is 4.6% of the native activity.) The ratio of slopes in eq 2 is found to be 2.01 ± 0.08 at 4° and 9945 rpm, in 0.5 PCEP. Extensive polydispersity of the aggregate molecular weight is ruled out by the linearity of the variation of ln c with x^2 seen in Figure 6.

These results indicate clearly that the thermodynamically

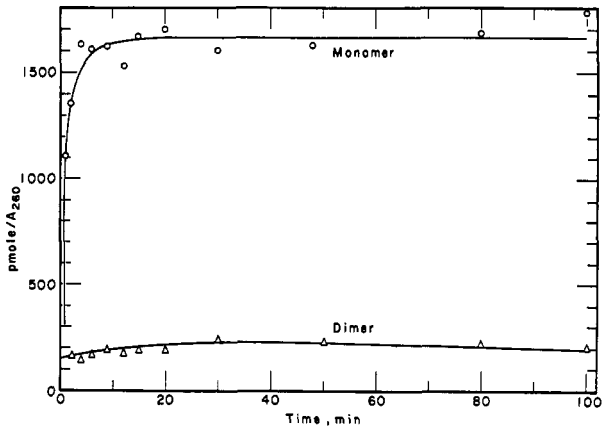

FIGURE 8: Charging kinetics of $tRNA_I^{Tyr}$ monomer and dimer. Each assay mixture was incubated at 37° and aliquots were taken at the indicated time. The synthetase used in this assay is stable when it is heated at 37° for up to 60 min prior to adding to the assay mixture.

perferred aggregate species is a dimer. One can, for example, try the assumption that aggregation is nonspecific, and take a single equilibrium constant for addition of each monomer unit to form trimer from dimer, tetramer from trimer, etc. Using the 4.6% residual activity as the per cent monomer present, one calculates that the weight-average molecular weight for this model should be 42.5 times the monomer value, far beyond the experimental ratio. We cannot exclude small percentages of higher aggregates, but there is clear thermodynamic preference for the dimer. Many of the observations of tRNA aggregation mentioned earlier show a range of aggregate sizes. The main difference between those experiments and ours is that our dimer is produced under annealing conditions, where the reaction is allowed to come to thermodynamic equilibrium.

SEDIMENTATION VELOCITY. The sedimentation coefficient of monomer and dimer were measured at 4° in 0.5 PCEP at 47,660 rpm, and corrected to water at 20° in the usual manner. Both materials sedimented as single boundaries. The measured coefficients are listed in Table I.

GEL FILTRATION. Figure 7 shows the results of Sephadex gel filtration of untreated (a) and heated (b) solutions of $tRNA^{Tyr}$. Heat treatment at 50° converts the bulk of the tRNA to an aggregate (dimer) eluting as a single band, and inactive in tyrosine acceptance. Heat treatment at 70° restores charging activity.

Properties of the Dimer. CHARGING KINETICS. One of the possible characteristics of the dimer is that it is actually chargeable, only more slowly than the monomer to account for its inactivity in the usual assay. We therefore measured the charging kinetics, using the procedure described by Söll *et al.* (1967). Figure 8 shows that the native $tRNA_I^{Tyr}$ reached full

TABLE I: Comparison of Properties of Monomer and Dimer.[a]

	Monomer	Dimer
$s_{20,w}$	4.04 ± 0.05	5.91 ± 0.05
M_{app}	25,400 ± 500	51,200 ± 1000

[a] All values measured in 0.5 PCEP at 4°.

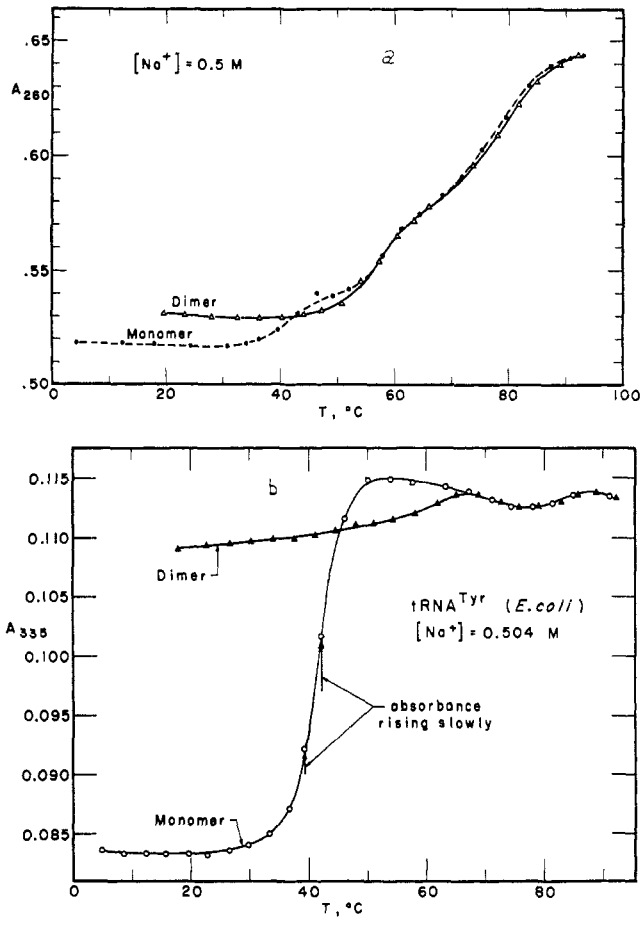

FIGURE 9: Melting curves of $tRNA_I^{Tyr}$ monomer and dimer in 0.5 PCEP. (a) 260-nm melting curves: monomer (○) and dimer (△). There is a slow downward drift of the absorbance between 45 and 51° in the melting of monomer. The dimer melts slowly, with absorbance drifting upward between 45 and 68°; 15 to 90 min is needed to obtain a steady absorbance reading. The curves were plotted by assuming that the monomer and dimer have the same absorbance at 92°. (b) 335-nm melting curves: monomer (○) and dimer (△). The temperature range of the upward drift in absorbance for the melting of monomer is a little lower than that measured at 260 nm. An upward drift in absorbance is observed for the dimer melting, as also observed at 260 nm. The absorbance was normalized to give equal values at 92° for the monomer and dimer.

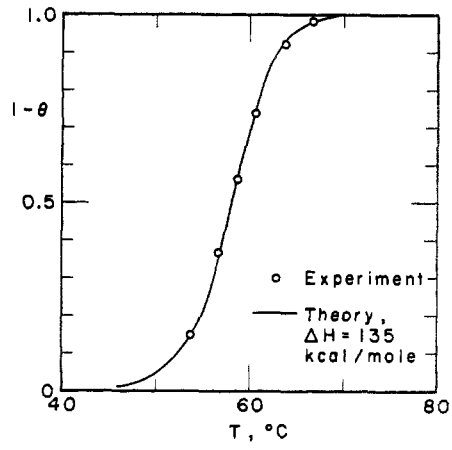

FIGURE 10: Theoretical and adjusted experimental dimer melting curve. See text for details.

activity in a few minutes; the dimer reached its low residual activity in the same time period. Both samples showed no significant increase in activity after further incubation. The stability of the aminoacyl-tRNA synthetase used for these assays was checked by heating at 37° prior to adding to the assay mixture. It was found that maximal charging of the monomer still occurred when the synthetase has been heated up to 60 min. Hence we conclude that the dimer is inactive, and the residual activity is due to rapidly charged monomer.

THERMAL TRANSITION CURVES. The monomer and dimer of $tRNA_I^{Tyr}$ differ substantially in their melting behavior. We measured transition curves both at 260 nm (Figure 9a) and at 335 nm (Figure 9b), the latter reflecting the absorbance of 4-thiouridine. The main difference between monomer and dimer is the absence in the latter of the transition with midpoint around 42° (in 0.5 M Na^+, Mg^{2+} absent, EDTA present). This transition has a relatively small optical change at 260 nm, but accounts for the major absorbance change at 335 nm. We have associated this effect with melting of the tRNA tertiary structure (P. E. Cole, S. K. Yang, and D. M. Crothers, paper in preparation). Its absence in the dimer indicates that in this case the native tertiary structure is not present, which is possibly the reason the dimer is inactive.

In the melting of both monomer and dimer measured at 260 nm, a second transition is observed with midpoint around 58°. This effect is clearly melting of the dimer structure, since very slow absorbance changes are observed through this temperature range, and it is at temperatures above 60° that slow reconversion to active monomer can be demonstrated (Figure 5). The reason one observes the transition in a preparation that is monomeric at low temperatures is that the sample converts partly to dimer in the range around 50°. Slow drifting of the absorbance is observed between 45 and 68°, so the melting curve depends on the rate of temperature increase.

Optical effects above 68° are due to melting of the secondary structure of the monomeric tRNA, presumably primarily the "cloverleaf" pattern. Samples that were originally monomer or dimer are both monomeric above this temperature, and their transition curves are identical.

The transition curves in Figures 9a and b allow one to rationalize the formation of dimers at 50°. At that temperature the melting of the native tertiary structure is complete, but melting of the dimer has barely begun. Therefore the cloverleaf produced by loss of tertiary structure is able to reduce its free energy by forming dimer. Dimer preparations were made at a concentration about 10 times higher than that of the transition curve in Figure 9a. This facilitates dimer formation both on kinetic and equilibrium grounds.

MELTING OF DIMERS BY THE TEMPERATURE-JUMP TECHNIQUE. Slow optical changes occur in the transition centered around 58° in Figure 8a; because of the slow reactivation kinetics (Figures 4 and 5) we can confidently associate the slow-absorbance component with dissociation of the dimer. We changed the temperature of the spectrophotometer cell quickly by switching the circulation from one constant temperature bath to another. The cell reaches its equilibrium temperature within 100 sec, and the equilibration of the dimer is considerably slower than this throughout most of its melting transition. Following a temperature jump the absorbance change separates into fast and slow components. The slow component is exponential within experimental error, and extrapolation back to the time of the temperature jump yields a value for the absorbance change associated with the slow exponential decay time. Summation of such changes up to each temperature

TABLE II: Kinetic and Thermodynamic Parameters for Dimerization of $tRNA_I^{Tyr}$.[a]

$\Delta H = -135 \pm 20$ kcal/mole	$k_a = 4 \times 10^2$ M^{-1} sec^{-1}, $T = 59°$
$E_a^{\ddagger} = -20 \pm 20$ kcal/mole	$k_d = 8 \times 10^{-4}$ sec^{-1}, $T = 59°$
$E_d^{\ddagger} = 115 \pm 20$ kcal/mole	$K = 5 \times 10^5$ M^{-1}, $T = 59°$

[a] $E_a^{\ddagger}$ and $E_d^{\ddagger}$ are the Arrhenius activation energies for the association and dissociation reactions, respectively.

produces a melting curve for the dimer, separated from other, faster, effects.

Figure 10 shows the thermal transition curve for the $tRNA_I^{Tyr}$ dimer, determined in this way. Because the transition becomes uncomfortably fast above 65°, the last points are less accurate than the others. Furthermore, in order to calculate a fractional conversion curve, we allowed adjustability, within the experimental error, of the total absorbance change through the transition. The adjustment was made to fit the curvature at the high temperature end of the theoretical melting curve expected for a dimer, derived below. We found that the dimer melting contributed a 3.8% increase of the absorbance at 260 nm.

Since the melting of the dimer produces a single exponential decay time, it can be adequately represented by a two-state model

$$2M \underset{k_d}{\overset{k_a}{\rightleftharpoons}} D \tag{3}$$

where M is monomer and D is dimer, k_a and k_d are the association and dissociation rate constants, repectively, and the dimerization equilibrium constant K is

$$K = k_a/k_d \tag{4}$$

Further, letting θ be the fraction of molecules present as dimer and C_T the total concentration of tRNA (expressed as moles per liter if all were monomer), we have

$$K = [D]/[M]^2 = \frac{\theta}{2(1-\theta)^2 C_T} \tag{5}$$

which relates θ to K and C_T.

From the van't Hoff equation, we have

$$\frac{d \ln K}{dT} = \frac{\Delta H}{RT^2} \tag{6}$$

where ΔH is the heat of dimer formation. Integrating eq 6 and combining with eq 5 yields

$$\ln KC_T = \frac{\Delta H}{R}(1/T_m - 1/T) \tag{7}$$

where T_m is the temperature at which $\theta = 0.5$. By adjusting ΔH, and using the experimental T_m, eq 5 and 7 can be used to produce a theoretical curve in agreement with experiment.

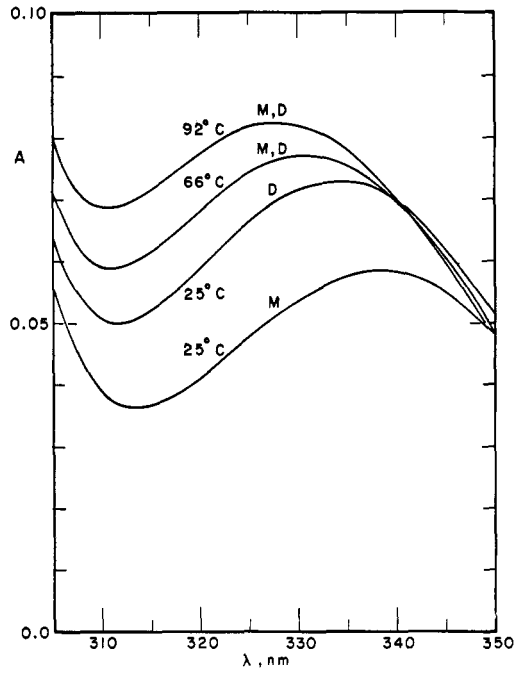

FIGURE 11: Absorbance spectra of $tRNA_I^{Tyr}$ monomer and dimer in 0.5 PCEP. Spectra were measured at 25, 66, and 92°. The absorbance of monomer (M) and dimer (D) were normalized to the same value at 92°.

The result is shown in Figure 10, for which $\Delta H = -135$ kcal/mole. Considering all the uncertainties in the analysis, we estimate that the enthalpy required to convert the dimer to monomer (the latter probably in the cloverleaf form, without tertiary structure) is 135 ± 20 kcal/mole.

RELAXATION KINETICS OF DIMER MELTING. The relaxation time τ for a bimolecular dimerization, eq 3, is

$$1/\tau = 4k_a[M] + k_d \tag{8}$$

Using eq 4 and the definition of θ yields

$$k_a = \frac{1}{\tau C_T[4(1-\theta) + 1/KC_T]} \tag{9}$$

Hence, measurement of τ, and knowledge of θ and KC_T from the transition curve, allows us to calculate k_a and hence k_d at each temperature. Results are shown in Table II. The activation energy of 115 ± 20 kcal per mole is in reasonable agreement with the value of 130 ± 15 estimated from the reactivation kinetics (Figure 5). The latter value refers to the conversion in the presence of Mg^{2+}, while the former was measured in 0.5 M Na^+. From the initial (concentration-dependent) rate of inactivation in Figure 3, we estimate $k_a = 5 \times 10^2$ M^{-1} sec^{-1} at $T = 50°$, agreeing with experimental error with the results in Table II. There is general agreement of kinetic parameters and temperature range of the transition as measured by optical methods or biochemical inactivation, and we conclude that the two methods measure the same process.

ABSORBANCE SPECTRA. Monomer and dimer differ in spectral properties at low temperature, as is apparent from the thermal transition curves measured at 260 and 335 nm (Figure 9). By about 66°, where the melting of dimer structure is essentially complete, the two transition curves converge. At this point the conformation is probably best approximated by the cloverleaf secondary structure model. Figure 11 shows

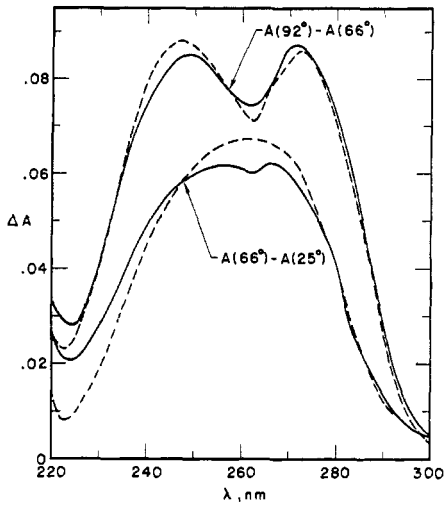

FIGURE 12: Thermal difference spectra of $tRNA_I^{Tyr}$ monomer and dimer in 0.5 PCEP. The absorbance of monomer and dimer were normalized to the same value at 92°. Difference spectra are plotted for monomer (dotted curves) and dimer (solid curves) at the indicated temperatures.

the main contrast, in percentage terms, between absorption of monomer and dimer: namely, the absorbance band due to thiouridine. Thiouridine in the monomer is considerably hypochromic with respect to dimer, both at 25°. This hypochromism of thiouridine is characteristic of native tRNAs (Seno *et al.*, 1969; P. E. Cole, S. K. Yang, and D. M. Crothers, paper in preparation), and its absence in the dimer clearly indicates the lack of native structure. At 66 and at 92°, preparations that were originally monomer or dimer have identical absorption spectra, reinforcing the conclusion that they have converted to the same (monomeric) form.

The spectral changes in the band around 260 nm are smaller in percentage terms, so we report the results in terms of thermal difference spectra, in other words the wavelength dependence of the difference in absorbance $A(T_2) - A(T_1)$ at temperatures T_2 and T_1. Figure 12 shows such data. The two curves of smaller amplitude refer to $T_2 = 66°$ and $T_1 = 25°$ (in 0.5 M Na^+) for monomer and dimer. The former temperature was chosen, because at 66° melting of the dimer is nearly complete and the monomer tertiary structure has been lost,

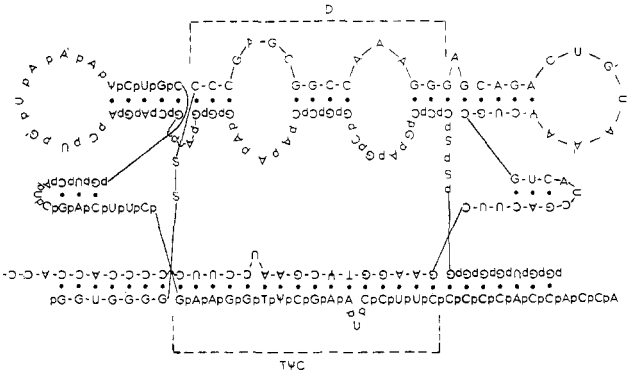

FIGURE 13: Proposed model for the dimer of tRNA (*E. coli*). The internucleotide link is indicated by a hyphen in one strand and by p in the other. Dimerization occurs through the dihydrouridine (D) and TΨC arms of the cloverleaf structure. The original sequence (Goodman *et al.*, 1968) should be consulted for identification of modified nucleotides.

while the main melting transition, that of cloverleaf, has barely begun. The similarity of the curves for monomer and dimer indicates that the number and composition of the base pairs formed in the dimer are similar to those formed in the monomer tertiary structure, each relative to the basic cloverleaf secondary structure.

The two upper curves, for $T_2 = 92°$ and $T_1 = 66°$ are virtually identical, as they should be if the monomer and dimer preparations have converted to the same (monomeric) form in this temperature range. The two peaks in the difference spectrum indicate melting of a highly G·C rich structure (Fresco *et al.*, 1963). The cloverleaf model for $tRNA_I^{Tyr}$ provides 17 G·C and 6 A·U pairs (including bonding in the extra arm), in qualitative agreement with the spectral observation. Comparison of the difference spectrum for melting of the dimer to cloverleaf ($A(66°) - A(25°)$) with that for melting of cloverleaf to coil ($A(92°) - A(66°)$) permits the conclusion that the extra base pairs formed in the dimer are less G·C rich than the base pairs in the cloverleaf secondary structure.

Discussion

Our results show that $tRNA_I^{Tyr}$ forms a dimer in solutions containing 0.5 M Na^+ but no Mg^{2+}, 50° being a convenient temperature for conversion to dimer. The heat of melting the dimer is about 135 kcal/mole, and the rate constant for dimer formation is three to four orders of magnitude slower than for dimerization of two complementary oligonucleotide strands. Melting of the dimer produces a fractional absorbance increase of 0.038 ± 0.005 at 260 nm, and the shape of the thermal difference spectra indicates that the extra pairing in the dimer is less G·C rich than in the cloverleaf structure of the monomer. The thiouridine absorbance is much more hypochromic in the monomer at low temperature than in the dimer. Finally, the dimer does not accept tyrosine in the usual charging assay.

The important question that remains is the structure of the dimer, especially the nature of the self-complementarity that enables two $tRNA^{Tyr}$ molecules to bond together. The structure we propose is that shown in Figure 13, involving interaction of the TψC and dihydrouridine regions of the two molecules. The dimer contains 10 more base pairs than the sum of two cloverleaf monomers; 6 of these come from self-complementarity in the TψC loop, and 4 from the dihydrouridine loop. Of the 10 extra pairs, 6 are G·C. Using the results of Fresco *et al.* (1963) on model RNA double helices and assuming that the bases that bond in the dimer have the average tRNA extinction coefficient, we calculate that formation of 10 pairs of 60% G·C composition should cause a fractional absorbance increase of 0.038 at 260 nm, in close agreement with experiment. Furthermore, since the thermal difference spectra indicate that dimer bonding (proposed at 60% G·C) is less G·C rich than the cloverleaf secondary structure (74% G·C), the model in this regard shows qualitative agreement with experiment. (The thermal difference spectrum cannot be used quantitatively, since it contains a fast kinetic component not ascribed to conversion of dimer to monomer. The fractional absorbance change of 0.038 was obtained from summation of slow kinetic effects.)

The measured enthalpy of dimer melting is 135 ± 20 kcal/mole. This represents a contribution of 13.5 kcal/mole of new base pairs formed in the dimer model, a value somewhat larger than observed for melting of double-helical poly(A)·poly(U)- (Krakauer and Sturtevant, 1968). However, G·C pairs may contribute more than A·U, and there may be substantial heat effects from the electrostatic interaction engendered by bring-

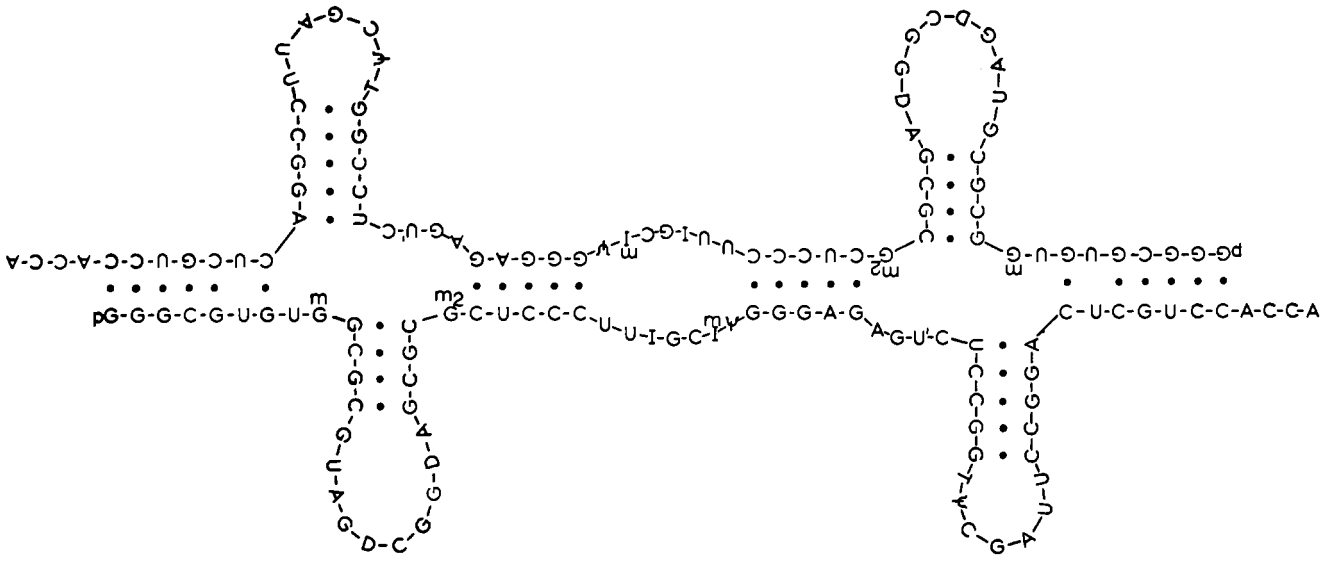

FIGURE 14: Model for the dimer of $tRNA_{1ab}^{Ala}$ (yeast) proposed by Loehr and Keller (1968).

ing the two tRNA molecules together. Certainly the model cannot be dismissed because the measured heat is a little larger than simple considerations would have predicted.

One feature of the model that bears on kinetic properties is the topological linking of the two strands together. Consideration of the spatial character of the dimer structure shown in Figure 13 makes it clear that the two monomers cannot be separated without opening the amino acid acceptor stem of at least one of them. We expect that this requirement would slow down both the association and dissociation reactions, and we use this feature of the model to account for the small dimerization rate constant in comparison with single-strand reactions. (The rate constant k_a in Table II is about 3000 times slower than for dimerization of single-stranded oligonucleotides (Craig *et al.*, 1971).) The exact mechanism of dimerization is clearly a complicated problem; we will not consider it in detail except to note that the apparent activation energy for dimer formation is negative. This means that the rate-limiting step does *not* occur after net breakage of base pairs in the monomer, since such a mechanism would provide a positive activation energy. To predict a negative activation energy, one must consider mechanisms in which any necessary breakage of base pairs in the monomer is slightly over compensated by formation of new pairs in the nascent dimer, all of this occurring before the rate-limiting step in dimer formation.

In our view the critical feature of $tRNA_I^{Tyr}$ (*E. coli*) that makes dimerization possible is the sequence in the TψC loop, this being -T-ψ-C-G-A-A-U-. The first six bases are self-complementary, permitting formation in the dimer of a continuous helix 16 base pairs long, with only the two uridines looped out of the structure. Such "looped out" defects are known to occur in synthetic polynucleotides, and are probably less destabilizing than a mismatching base pair. We made a rough theoretical calculation, the details of which are unimportant here, of the stability expected from a dimer based only on interaction through the TψC loop, and found a predicted T_m of 52° compared with the observed value of 58°. We expect that the proposed pairing in the dihydrouridine loop contributes additional stability, but the major contributor is self-complementarity of the TψC loop. (Theoretical stability calculations, inaccurate at best with tRNA, become sheer guesswork for the dimer structure diagrammed in Figure 13, because we have no way of evaluating the free-energy contribution of the large and complicated ring that is formed.)

Hence, according to our model, only tRNAs that have the sequence -T-ψ-C-G-A-A- (or -T-ψ-C-G-A-G-, if a G·T pair is assumed) can show strong dimerization by this mechanism. Examples are $tRNA_{II}^{Tyr}$ (*E. coli*), $tRNA^{Met}$ (*E. coli*) (Cory *et al.*, 1968), $tRNA_3^{Leu}$ (yeast) (Kowalski *et al.*, 1971), and $tRNA_2^{Ser}$ (yeast) (Zachau *et al.*, 1966). In agreement with our model, dimers of $tRNA_3^{Leu}$ (Kowalski and Fresco, 1971a) and nonchargeable aggregates of $tRNA_{II}^{Ser}$ (yeast) have been observed (Adams and Zachau, 1968; Zachau, 1968). According to the results of Cole (1971), extensive dimerization of $tRNA^{fMet}$, $tRNA^{Val}$, and $tRNA^{Phe}$, all from *E. coli*, does not occur, since thermal transition curves of the kind shown in Figure 1 are much more reversible than is found for $tRNA_I^{Tyr}$ (*E. coli*). Our model predicts that these three tRNAs would not dimerize by the mechanism we propose for $tRNA_I^{Tyr}$.

Our model also predicts that $tRNA^{Ala}$ (yeast) should not dimerize, yet the existence of dimers has been clearly demonstrated (Loehr and Keller, 1968). However, that dimer is chargeable, and we conclude that dimerization occurs by a different mechanism. The structure proposed by Loehr and Keller is shown in Figure 14; there are two difficulties with their proposal. First, it does not predict that specifically $tRNA^{Ala}$ (yeast), and not other species, should dimerize in this way, since the same structure can be drawn for any tRNA. Second, there is no indication of the thermodynamic driving force for dimer formation, since the number of pairs in the dimer is no greater than the sum of monomers. Under these conditions, one would expect the entropy gain on separation to predominate, and that the tRNA would exist as monomers.

To overcome these difficulties, we propose the modification of their model shown in Figure 15. "Tertiary" base pairing is used to form a helix in the anticodon region, with participation of bases from the dihydrouridine loop. We found that the structure in Figure 15 could be built using space-filling Corey–Pauling–Koltun models. A dislocation in the helix, including a translation of the helix axis, is necessary to allow the -mI-ψ- section to bridge three base pairs. The structure proposed is highly specific for the sequence in $tRNA^{Ala}$ (yeast), it provides a thermodynamic basis for dimerization and accounts for the

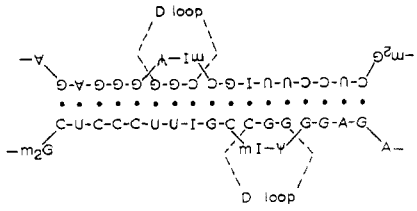

FIGURE 15: Proposed tertiary structure in the anticodon loop of the model shown in Figure 14.

observation of Loehr and Keller that the anticodon region becomes resistant to nuclease attack upon dimerization. In this case, unlike $tRNA_I^{Tyr}$ (*Escherichia coli*), the tertiary structure of the dimer is evidently sufficiently like that of monomer to allow charging.

Finally, we should note that there are doubtless other mechanisms for tRNA aggregation. In particular, one can expect a wide range of products when the aggregation occurs under nonequilibrium conditions, such as addition of Mg^{2+}-containing neutral buffer to a solution of tRNA at low pH. In such cases, kinetic factors will play a predominant role in determining the products, and one can expect a complex mixture. In general, annealing conditions should yield simpler results.

References

Adams, A., Lindahl, T., and Fresco, J. R. (1967), *Proc. Nat. Acad. Sci. U. S. 57*, 1684.

Adams, A., and Zachau, H. G. (1968), *Eur. J. Biochem. 5*, 556.

Armstrong, D. J., Burrows, W. J., Skoog, F., Roy, K. L., and Söll, D. G. (1969), *Proc. Nat. Acad. Sci. U. S. 63*, 834.

Brown, G. L., and Zubay, G. (1960), *J. Mol. Biol. 2*, 287.

Casassa, E. F., and Eisenberg, H. (1964), *Advan. Protein Chem. 19*, 287.

Cole, P. E. (1971), Thesis, Yale University.

Cory, S., Marcker, K. A., Dube, S. K., and Clark, B. F. C. (1968), *Nature (London) 220*, 1039.

Craig, M. E., Crothers, D. M., and Doty, P. (1971), *J. Mol. Biol. 62*, 383.

Fresco, J. R., Klotz, L. C., and Richards, E. G. (1963), *Cold Spring Harbor Symp. Quant. Biol. 28*, 83.

Goodman, H. M., Abelson, J., Landy, A., Brenner, S., and Smith, J. D. (1968), *Nature (London) 217*, 1019.

Hampel, A., Cherayil, J., and Bock, R. M. (1971), *Biochim. Biophys. Acta 228*, 482.

Johnson, J. S., Kraus, K. A., and Scatchard, G. (1954), *J. Phys. Chem. 58*, 1054.

Kowalski, S., and Fresco, J. R. (1971), *Science 172*, 384.

Kowalski, S., Yamane, T., and Fresco, J. R. (1971), *Science 172*, 385.

Krakauer, H., and Sturtevant, J. M. (1968), *Biopolymers 6*, 491.

Lipsett, M. N., and Doctor, B. P. (1967), *J. Biol. Chem. 242*, 4072.

Loehr, J. S., and Keller, E. B. (1968), *Proc. Nat. Acad. Sci. U. S. 61*, 115.

Nishimura, S., Harada, F., Narushima, U., and Seno, T. (1967), *Biochim. Biophys. Acta 142*, 133.

RajBandary, U. J., Chang, S. H., Gross, H. J., Harada, F., Kimura, F., and Nishimura, S. (1969), *Fed. Proc., Fed. Amer. Soc. Exp. Biol. 28*, 409.

Röschenthaler, R., and Fromageot, P. (1965), *J. Mol. Biol. 11*, 458.

Scheffler, I. E., Elson, E. L., and Baldwin, R. L. (1968), *J. Mol. Biol. 36*, 291.

Schleich, T., and Goldstein, J. (1964), *Proc. Nat. Acad. Sci. U. S. 52*, 744.

Seno, T., Kobayashi, M., and Nishimura, S. (1969), *Biochim. Biophys. Acta 174*, 71.

Söll, D. G., Cherayil, J. D., and Bock, R. M. (1967), *J. Mol. Biol. 29*, 97.

Tanford, C. (1961), Physical Chemistry of Macromolecules, New York, N. Y., Wiley.

Zachau, H. G. (1968), *Eur. J. Biochem. 5*, 559.

Zachau, H. G., Dütting, D., and Feldman, H. (1966), *Angew. Chem. Int. Ed. 5*, 422.